



Helicopters Turboshift Engines Parameters
Identification Using Neural Network
Technologies Based on the Kalman Filter

Serhii Vladov, Yuri Shmelov, Ruslan Yakovliev and
Maryna Petchenko

EasyChair preprints are intended for rapid
dissemination of research results and are
integrated with the rest of EasyChair.

August 7, 2023

Helicopters Turboshaft Engines Parameters Identification Using Neural Network Technologies Based on the Kalman Filter

Serhii Vladov¹[0000-0001-8009-5254], Yuriy Shmelov¹[0000-0002-3942-2003], Ruslan Yakovliev¹[0000-0002-3788-2583] and Maryna Petchenko²[0000-0003-1104-5717]

¹ Kremenchuk Flight College of Kharkiv National University of Internal Affairs, Peremohy Street, 17/6 39605, Kremenchuk, Ukraine

² Kharkiv National University of Internal Affairs, L. Landau Avenue, 27, 61080, Kharkiv, Ukraine
ser26101968@gmail.com

Abstract. The work is a continuation of the research devoted to the development of a multidimensional Kalman filter connected at the output of the built-in helicopter's turboshaft engines mathematical dynamic model to improve the accuracy of helicopters turboshaft engines parameters identification and achieve high quality automatic control. The main difference is the use of radial basis functions neural networks, in which the multivariate Kalman filter is a training algorithm. The work illustrates well-known mathematical expressions underlying of optimal multidimensional filtering algorithms. The methods of mathematical modeling in the Matlab environment tested the proposed algorithms. The simulation results showed that the use of neural networks trained by the multidimensional Kalman matrix filter as part of the model of helicopters turboshaft engines built into the automatic control system allows achieving high indicators of the accuracy of identifying the parameters of helicopters turboshaft engines automatic control system – up to 0.9975, then in practical analogues.

Keywords: Helicopter Turboshaft Engine, Neural Network, Kalman Filter, Training, Accuracy.

1 Introduction

Aircraft helicopters turboshaft engines (TE) are complex nonlinear systems, the characteristics of which have a significant scatter [1]. The quality of the built-in mathematical models of helicopters TE that are part of the automatic control system (ACS) [2] largely determines the quality of control and the possibility of using modern mathematical apparatus for the synthesis of ACS, as well as operating tools [3]. Satisfaction with the requirements for the reliability and quality of regulation of helicopters TE is possible only by expanding the functionality of the controls, in particular, endowing them with the ability to quickly adapt to changes in the characteristics of helicopters TE and external conditions. The change in the characteristics of helicopters TE is due

to many reasons, the main of which are [4]: parameters technological spread due to tolerances for the manufacture and units' assembly; deviation in the similarity of modes under various external operating conditions; change in characteristics in the process of resource development (failures and units wear).

External interference is caused by a wide range of external destabilizing factors that affect the engine during operation, causing additional errors and reducing the resource: a wide range of operating temperatures ranging from -50 to 100 °C; mechanical shocks, linear acceleration and vibration corresponding to overloads of 10...15 tons or more; instability of ACS power supplies, and also due to the impact of pulses, which are almost twice the nominal value; electromagnetic interference; pressure pulsations with an amplitude of 20...90 % of the upper limit; chemically aggressive impurities in the environment, etc.

Solving the task of ACS adaptation, as well as real-time condition monitoring and failure diagnostics, inevitably requires the use of identification methods using artificial intelligence tools (for example, neuron networks) [5]. In this case, the structure and accuracy of the applied mathematical model are determined by the nature of the problem for which they are applied.

2 Related Works

The process of ensuring the stability of engine parameters in all operating modes is one of the priority tasks at the helicopters TE ACS operation mode. At the same time, the ACS performs the following main functions: engine start automatic control, quick transition to other operating modes when controlling the engine or in case of a sharp change in external conditions, maintaining the specified engine operation mode or changing it in accordance with control programs, preventing the engine from entering dangerous operating modes. Of particular difficulty are the starting modes and engine transient modes operation under conditions of external and internal interference [6, 7].

To implement the above functions, a necessary condition is to obtain reliable data on the current parameters of helicopters TE at flight modes (in real time), such as fuel consumption, temperature, pressure, gas generator and free turbine rotor speeds, etc. [8, 9]. Modern helicopters TE ACS operates under interference conditions both in the built-in model channel (due to model inaccuracy and interference in the communication channel) and in the measurement channel (due to sensor error and communication channel interference). That's why an urgent task is to ensure the accuracy of parameter identification, taking into account calculated data obtained using the built-in model, and data from current on-board measurements. The identification accuracy is determined by the methods used [10, 11].

In connection with the foregoing, the aim of the work is to improve the accuracy of helicopters TE parameters identification by using neural network technologies, namely, training the multidimensional Kalman filter at the output of the built-in mathematical dynamic model of identification, develop on the basis of engine's dynamic and throttle characteristics, which makes it possible to identify the parameters and simulate the operation of the engine in stationary and dynamic modes [12, 13]. It should be noted that

this study is a continuation of research in the field of development of helicopters TE intelligent on-board automatic control systems, in which it is proposed to integrate a multidimensional Kalman filter [14].

3 Materials and Methods

Multidimensional filtering is carried out according to three helicopters TE thermo-gas-dynamic parameters, which are recorded on board the helicopter: n_{TC} – rotor r.p.m.; n_{FT} – free turbine rotor rotational speed; T_G – gas temperature in front of the compressor turbine, recorded on board of the helicopter, reduced to absolute parameters, according to the theory of gas-dynamic similarity [15] (table 1).

Table 1. Fragment of the training sample during the operation of helicopters TE (on the example of TV3-117 TE) [15].

Number	n_{TC}	n_{FT}	T_G
1	0.932	0.929	0.943
2	0.964	0.933	0.982
3	0.917	0.952	0.962
4	0.908	0.988	0.987
5	0.899	0.991	0.972
6	0.905	0.987	0.979
7	0.923	0.972	0.983
8	0.948	0.966	0.989
9	0.962	0.952	0.997
...
256	0.953	0.973	0.981

According to [14], the recursive Kalman filter for the task posed is the most accurate and convenient in modeling, having the necessary properties of adaptation – self-correction in the process of filtering data. Adaptation is based on the application of a variable optimal Kalman coefficient obtained at the current moment when solving the problem of minimizing the mathematical expectation of the squared error of the identified parameter, taking into account the error at the previous moment (which determines the recurrence of the obtained relations) [14, 16]. Kalman filters are used for ergodic processes operating under noise conditions, characterized by a known time-independent dispersion and zero mathematical expectation [17].

To prove the ergodicity of the process, the feasibility of the Slutsky condition was checked, according to which the autocovariance function of the ergodic process should tend to zero as the lag value increases [14]. The research results showed the correctness of the hypothesis about the ergodicity of the observed processes. The analysis results for n_{TC} , n_{FT} , T_G are shown in fig. 1–3.

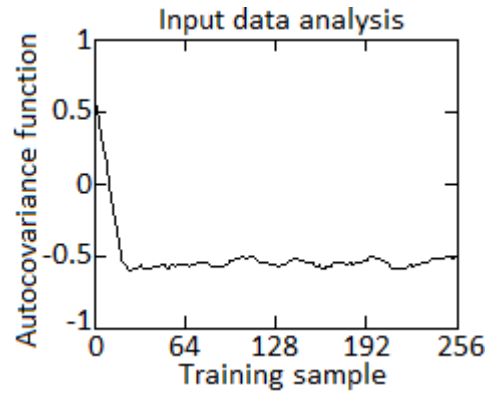


Fig. 1. Diagram of the autocovariance function for nrc (author's research).

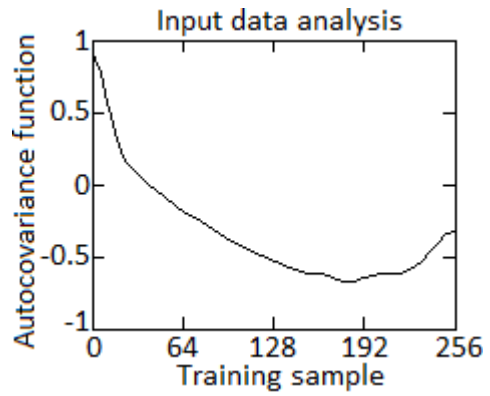


Fig. 2. Diagram of the autocovariance function for nFT (author's research).

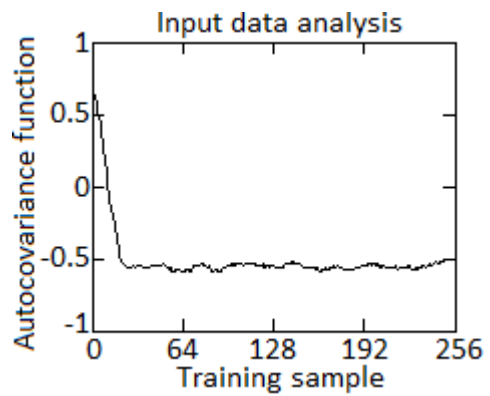


Fig. 3. Diagram of the autocovariance function for T_G (author's research).

According to [14], the analysis of real noises obtained from the data of flight tests of the TV3-117 engine showed that all of them are characterized by zero mathematical expectation, constant dispersion, and the same spectra in the study of one long-duration sample and several samples. Thus, the hypothesis of ergodicity of the processes under consideration was again confirmed, since the values of the mathematical expectation and variance are the same both in time and in the number of realizations. The application of the Pearson criterion showed the normal distribution of noise. All this allows us to draw a conclusion about the further possibility of using Kalman filters (including neural networks trained using the Kalman filter) for this class of processes [18]. In the identification problem using the optimal Kalman filtering, according to [14, 16], it is required at the current time to eliminate the error as much as possible both in the model channel (the predicted value of the identified parameter) and in the measurement channel (current sensor readings) for the four parameters under consideration. For this, a recursive matrix relation is used, which makes it possible to determine the matrix of the square of the covariance error over all coordinates [19]:

$$\mathbf{E}_k^2 = \mathbf{E}_{k-1}^2 + \boldsymbol{\sigma}_\xi^2; \quad (1)$$

where \mathbf{E}_k^2 – column vector of the squared error of the covariance in the coordinates of the n_{TC} , n_{FT} , T_G at the k -th step, $\boldsymbol{\sigma}_\xi^2$ – matrix of model variances in the coordinates of the n_{TC} , n_{FT} , T_G .

The solution of the \mathbf{E}_k^2 minimization problem allows us to determine the elements of the matrix of the Kalman coefficient:

$$\mathbf{K}_k = \mathbf{E}_k^2 [\mathbf{E}_k^2 + \boldsymbol{\sigma}_\eta^2]^{-1}; \quad (2)$$

where \mathbf{K}_k – column vector of the Kalman coefficient for the coordinates of the n_{TC} , n_{FT} , T_G at the k -th step, is the variance matrix of the meter (sensor) in the matrix of model variances for the coordinates of the n_{TC} , n_{FT} , T_G .

Identification of parameters (obtaining an optimal estimate) is carried out through a column vector of Kalman coefficients, which determines in matrix form the ratio of the calculated (model) and measured components in the optimal values of the identified parameters:

$$\mathbf{X}_k^{opt} = \mathbf{X}_k (1 - \mathbf{K}_k) + \mathbf{K}_k \mathbf{Z}_k; \quad (3)$$

where \mathbf{X}_k^{opt} – column vector of optimal estimates of coordinates n_{TC} , n_{FT} , T_G at the k -th step; \mathbf{X}_k – column vector of model values of coordinates n_{TC} , n_{FT} , T_G , calculated at the k -th step; \mathbf{Z}_k – column vector of coordinates n_{TC} , n_{FT} , T_G measured by sensors at the k -th step.

It should be noted that the problem solved using Kalman filtering is not a smoothing problem, but an identification problem [20]. The Kalman filter is not designed for smoothing data from the sensor, but is aimed at obtaining the closest to the real coordinates n_{TC} , n_{FT} , T_G , the values of their optimal estimates at the current time, obtained

under conditions of external and internal interference in the channels of the built-in model and measurements and recorded in the column vector \mathbf{X}_k^{opt} .

In order to implement the considered method as part of the onboard neural network expert system for monitoring helicopters TE operational status [21] or in the modified closed onboard helicopters TE ACS [2, 15], as well as to increase the accuracy of helicopters TE parameters identification compared to [14], it is proposed to implement a multidimensional filter Kalman using neural networks.

Neural network training using the multidimensional Kalman filter [22] is the problem of estimating the true state of some unknown “ideal” neural network that provides zero mismatch, under states, in this case, the values of the weights of the neural network $w(k)$ are taken, and under the mismatch, the current error training $e(k)$. The dynamic training process of a neural network can be described by a pair of state-space equations, one of which is a process model representing the evolution of the weight vector under the influence of a random process $\zeta(k)$, which is considered white noise with zero mathematical expectation and the known diagonal covariance matrix Q :

$$w(k+1) = w(k) + \zeta(k). \quad (4)$$

The output equation is a linearized neural network model (5) at the k -th step, noisy with a random process $Q(k)$, which is considered to be white noise with zero mathematical expectation and a known diagonal covariance matrix R :

$$h(k) = \frac{\partial y(w(k), v(k), x(k))}{\partial w} + \zeta(k); \quad (5)$$

where $w(k)$ – neural network weights, $v(k)$ – neurons postsynaptic potentials, $x(k)$ – network input values. The instantaneous values of the derivatives $\frac{\partial y}{\partial w}$ are calculated using the backpropagation method. Mismatch $e(k)$ is calculated according to the expression:

$$e(k) = t(k) - y(k); \quad (6)$$

where $t(k)$ – neural network target value, $y(k)$ – neural network actual output, calculated according to the expression:

$$y(k) = g \left(\sum_j w_j^{(2)} f \left(\sum_j w_{ji}^{(1)} x_i \right) \right); \quad (7)$$

where $w^{(1)}$ – hidden layer neurons weights, $f(\bullet)$ – hidden layer neurons activation functions, $w^{(2)}$ – output layer neurons weights, $g(\bullet)$ – output layer neurons activation functions.

Before training, the neural network goes through the initialization stage. The covariance matrices of measurement noise $R = \eta \cdot I$ and dynamic training noise $Q = \mu \cdot I$ are

set, the size of the matrices is $L \times L$ and $N \times N$, respectively, where L – output neurons number, N – neural network weight coefficients number. The coefficient η has the meaning of the training rate, in this work according to [22] $\eta = 0.001$, the coefficient μ determines the measurement noise; in this work, according to [22], $\mu = 10^{-4}$. Also, a single covariance matrix P of size $N \times N$ and a zero-measurement matrix H of size $L \times N$ are set at the initialization stage. The training stage is performed online, the neural network correction weights is sequentially performed for each example of the training sample. At the k -th step, the following actions are performed:

1) A neural network output new value $y(k)$ is calculated according to (4), a “forward pass” of the neural network is performed.

2) A "reverse pass" of the neural network is performed: the derivatives are calculated using the backpropagation method $\frac{\partial y}{\partial w_i}$, $i = \overline{1, N}$. This is done using the same technique as in the error backpropagation method, but the local gradients for the output neurons are set not to the current error $e(k)$, but to the constant 1, which, with all the same calculations, provides the neural network outputs Jacobians values $\frac{\partial y}{\partial w}$ instead

of gradients $\frac{\partial (e(k))^2}{\partial w}$ because $\frac{\partial (e(k))^2}{\partial w} = 2e(k) \frac{\partial y}{\partial w}$. Observation matrix $H(k)$ is formed:

$$H(k) = \left[\frac{\partial y}{\partial w_1} \quad \frac{\partial y}{\partial w_2} \quad \dots \quad \frac{\partial y}{\partial w_N} \right]^T. \quad (8)$$

3) The current error of the network operation $e(k)$ is determined according to (6), a deviation matrix $E(k)$ of size $1 \times L$ is formed:

$$E(k) = [e(k)]. \quad (9)$$

4) New values of the neural network weights $w(k+1)$ and correlation matrix $P(k+1)$ are calculated according to the expressions:

$$K(k) = P(k)H(k)^T [H(k)P(k)H(k)^T + R]^{-1}; \quad (10)$$

$$P(k+1) = P(k) - K(k)H(k)P(k) + Q; \quad (11)$$

$$w(k+1) = w(k) + K(k)e(k); \quad (12)$$

where $K(k)$ – Kalman gain matrix, its dimension is $N \times L$.

Actions 1 – 4 are performed for all elements of the training sample. The correlation matrix P updated at each clock cycle contains second-order information about the error

surface, which provides the extended Kalman filter method with an advantage over first-order training methods such as gradient descent and its modifications.

4 Experiment

Based on [14], a neural network of radial basis functions (RBF) with 5 inputs is taken as a neural network, three of which are responsible for the input parameters n_{TC} , n_{FT} , T_G , and two specify the model error and the measurement error (fig. 4).

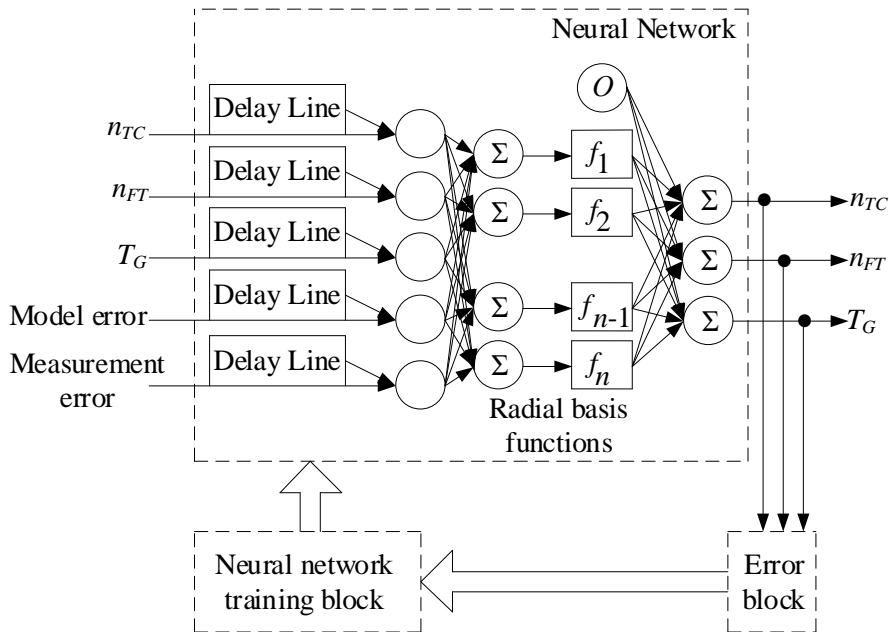


Fig. 4. Neural network diagram (author's research).

It is known that RBF-networks model an arbitrary non-linear function using only one intermediate layer, thereby eliminating the need to decide on the number of layers [23, 24]. Secondly, the parameters of the linear combination in the output layer can be optimized using well-known linear optimization methods that are fast and do not suffer from local minimum that interfere with training using the backpropagation algorithm. Therefore, the RBF-network trains very quickly – an order of magnitude faster than using the backpropagation algorithm.

In order to determine the optimal number of neurons in the hidden layer, an experimental dependence $E = f(N)$ was constructed, shown in fig. 5, where E – neural network training error; N – number of neurons in the hidden layer (it is assumed that the number of neurons in the input layer is 5, in the output layer is 3) [25].

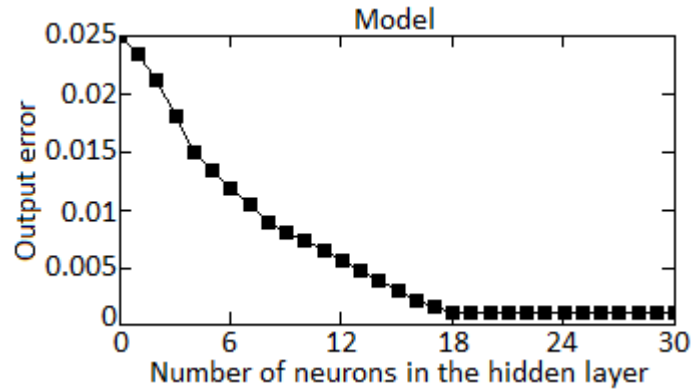


Fig. 5. Neural network training error diagram the number of neurons in the hidden layer (author's research).

As can be seen from fig. 5, with 18 neurons in the hidden layer, the smallest training error of the neural network is achieved, that is, the optimal structure of the neural network is 5–18–3.

The neural network training was carried out on a personal computer with an AMD Ryzen 5 5600 6-Core Processor 3.50 GHz CPU of the Zen 3 architecture, 32 GB of DDR-4 RAM and an Nvidia GeForce RTX 3060 GPU times compared to training on the CPU. To control of neural network training, we used the accuracy metric and the loss function, which was chosen as categorical entropy [26]. The experiment was carried out in laboratory conditions. At the same time, it was proved that under the conditions of on-board implementation, this method can be easily implemented using the 64-bit Intel Neural Compute Stick 2 neuroprocessor [27]. Diagrams of the dependence of the change in these values on the number of the epoch of network training are shown in fig. 6.

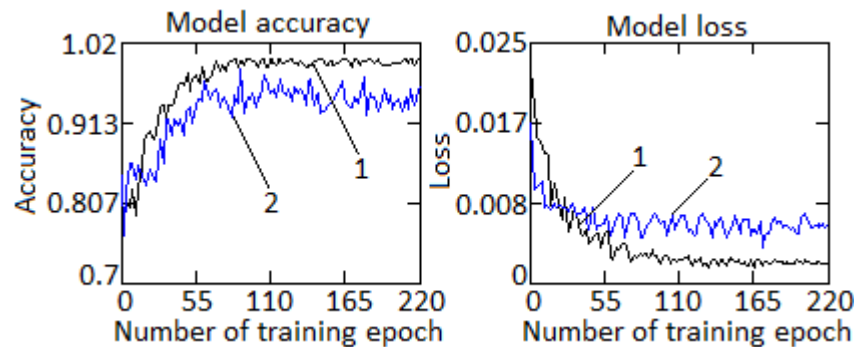


Fig. 6. Diagrams of changes in accuracy and loss when a neural network training: 1 – train, 2 – test (author's research).

As can be seen from fig.6, the accuracy indicator approaches one, and loss indicator – tends to zero, which indicates the high accuracy of the model and its minimal error [28, 29].

Table 2 contains the values of training and testing errors, as well as the training time, for various training algorithms, from which it can be seen that for the task at hand, the RBF-network training algorithm based on the multidimensional Kalman filter significantly outperforms other RBF-network training algorithms in terms of convergence rate (number of epochs) and identification accuracy.

Table 2. RBF-network training results (author's research).

Training algorithm	Identification error	Number of training epochs	Training time, s
Backpropagation algorithm	0.034	283	14
Quasi Newton algorithm [30]	0.031	275	12
Q-learning [31]	0.029	272	12
Genetic algorithm combination method [32]	0.027	268	11
Expectation-maximization algorithm [33]	0.026	264	11
Gradient algorithm [34]	0.018	247	8
Multidimensional Kalman filter [14, 22]	0.009	220	3.25

5 Results

Similarly, to [14], the task of developing multidimensional Kalman filtering algorithms using neural network technologies was solved on the basis of a model experiment in the Simulink interactive environment, which allows building dynamic models of the researched control objects based on block diagrams in the form of directed diagrams [34, 35].

Its main advantages are the variety of built-in libraries, including those included in the Matlab environment, visibility and ease of modeling, the ability to monitor the system operational status in real time, and the convenience of an interface that makes it easy to influence the designed algorithm and model experiment [36].

The task of developing an algorithm is reduced to modeling mathematical expressions (1) – (3) to calculate the specified values at each step. Calculations in the multidimensional Kalman filtering algorithms were based on the dispersions of the model and sensors along the coordinates n_{TC} , n_{FT} , T_G , obtained by statistical processing at flight test data of the TV3-117 TE.

The generalized block diagram of the model of the multidimensional Kalman filter, which performs real-time simultaneous identification by three coordinates of n_{TC} , n_{FT} , T_G , is shown in fig. 7.

A detailed functional diagram of filtering along one coordinate is taken from [14] and is shown in fig. 8.

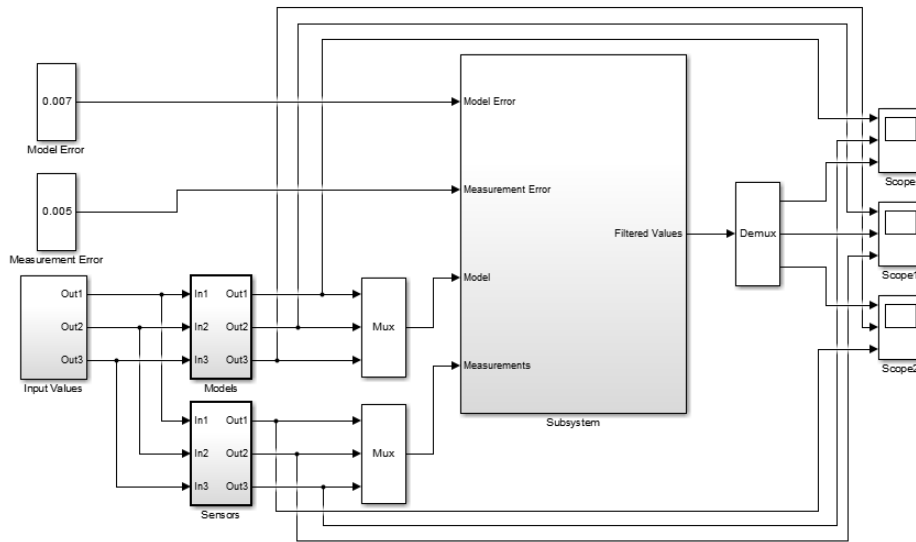


Fig. 7. Generalized block diagram of the multidimensional Kalman filter in Simulink (author's development based on [14]).

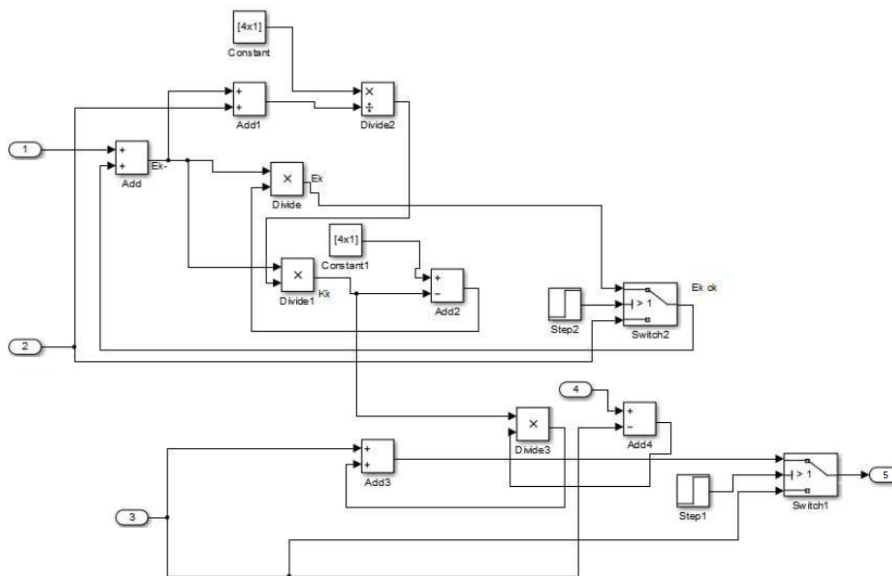


Fig. 8. Single coordinate filtering block diagram in Simulink [14]: 1 – model error, 2 – measurement error, 3 – model, 4 – measurement, 5 – filtered value.

Similarly, to [14], in the model experiment, the values of the coordinates of the column vector of the readings of the sensors Z_k under noise conditions were modeled by superimposing several types of noise on the calculated values: gaussian noise; real noise extracted from experimental data obtained during flight tests of the TV3-117 engine for the considered modes and types of input signals; several high frequency sinusoids; combined noise obtained by superimposing several high-frequency sinusoids on real noise. The results of filtering under the action of combined noises when applying input signals that provide a change in the identified values in the entire operating range for various input signals (acceleration – operating mode – reset) along one coordinate are shown in fig. 9, 10, where: 1 – change in time of the coordinates of the column vector \mathbf{X}_k – calculated (model) values of n_{TC}, n_{FT}, T_G ; 2 – change in time of the coordinates n_{TC}, n_{FT}, T_G of the column vector \mathbf{Z}_k – measured by the sensors of the values of the coordinates n_{TC}, n_{FT}, T_G ; 3 – change in time of the coordinates of the column vector \mathbf{X}_k^{opt} – optimal estimates of the coordinates n_{TC}, n_{FT}, T_G .

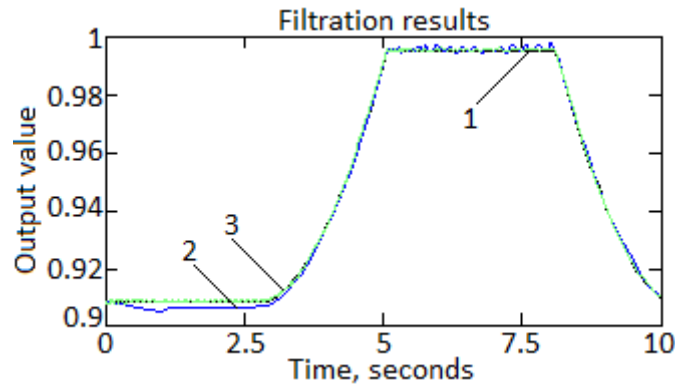


Fig. 9. The results of applying the multidimensional Kalman filter in the injectivity modes (reset under conditions of combined noise) (author's research).

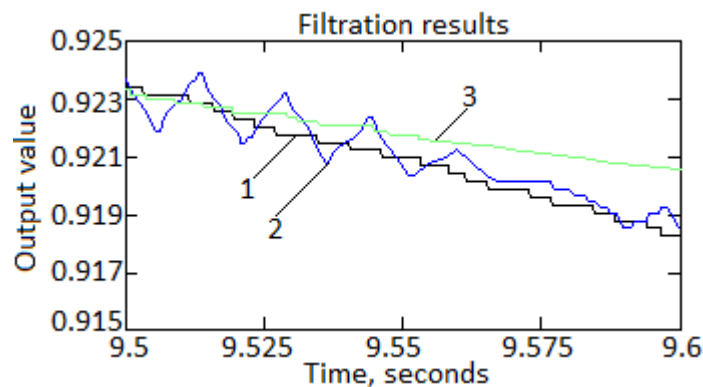


Fig. 10. The results of applying the multidimensional Kalman filter in the operating mode under conditions of combined noise (author's research).

6 Discussions

Researches have shown that the relative error of the signals at the output of the multidimensional Kalman filter neural network model for all researched coordinates n_{TC} , n_{FT} , T_G does not exceed 0.25 %, which corresponds to the specified technical requirements for the accuracy of identification algorithms. The results obtained indicate a two-fold decrease in the error of signals in the output of the multidimensional Kalman filter neural network model compared to the results obtained in [14]. The developed the multidimensional Kalman filter neural network model operates both in static and dynamic modes under the influence of "hard" external and internal disturbances in a wide range of helicopter TE operating modes.

Table 3 shows the results of a comparative analysis of the identification of the parameters of TV3-117 TE at three coordinates n_{TC} , n_{FT} , T_G by determining errors of the 1st and 2nd kind. It follows from Table 3 that the use of the multidimensional Kalman filter neural network reduces errors by an average of 20 % compared to the results obtained in [14].

Table 3. Identification 1st and 2nd kind errors calculation results (author's research).

Identification method based on multidimensional Kalman filter	Probability of error in parameter identification					
	n_{TC}		n_{FT}		T_G	
	Type 1st error	Type 2nd error	Type 1st error	Type 2nd error	Type 1st error	Type 2nd error
Without the use of neural networks [14]	0.84	0.63	0.85	0.64	0.79	0.58
Using neural networks	0.62	0.38	0.63	0.41	0.56	0.33

7 Conclusions

1. The method for helicopters turboshaft engines parameters identification using the multidimensional Kalman filter has been further developed, which differs from the existing one in that due to the use of radial basis functions neural network, it has increased the accuracy of helicopters turboshaft engines parameters identification with an accuracy of 0.9975.

2. The method of radial basis functions neural network training has been improved, which, due to the use of a training algorithm based on the multivariate Kalman filter, has reduced the identification error from 0.034 to 0.009 (3.4 to 0.9 %), the number of training epochs from 283 to 220, the training time from 14 to 3.25 seconds, which is critical in terms of on-board implementation.

3. It is proved that the errors of the 1st and 2nd implementations of the method for helicopters turboshaft engines parameters identification using the multidimensional Kalman filter neural network model did not exceed 0.63 % and 0.41 %, respectively, while for the classical method (multidimensional Kalman filter direct application [14]) they amounted to 0.85 % and 0.64 %, respectively. The obtained results prove that the

use of the multidimensional Kalman filter neural network filter will allow 25 % more accurate helicopters turboshaft engines parameters identification at the helicopter flight mode.

4. The prospect for further research is testing the developed multidimensional Kalman filter neural network model in the closed control loop of the modified closed onboard helicopters turboshaft engines automatic control system [2, 15], the onboard neural network expert system for monitoring helicopters turboshaft engines operational status [21] and a comparative analysis of the results obtained with the results of applying the element-by-element model and bench and flight test data in similar modes.

References

1. Zeng, J., Cheng, Y.: An Ensemble Learning-Based Remaining Useful Life Prediction Method for Aircraft Turbine Engine. *IFAC-PapersOnLine* 53(3), 48–53 (2020). <https://doi.org/10.1016/j.ifacol.2020.11.00>
2. Vladov, S., Shmelov, Y., Yakovliev, R.: Helicopters Aircraft Engines Self-Organizing Neural Network Automatic Control System. *The Fifth International Workshop on Computer Modeling and Intelligent Systems (CMIS-2022)*, May, 12, 2022, Zaporizhzhia, Ukraine. *CEUR Workshop Proceedings* 3137, 28–47 (2022). <https://doi.org/10.32782/cmisis/3137-3>
3. Yildirim, M. T., Kurt, B.: Aircraft Gas Turbine Engine Health Monitoring System by Real Flight Data. *International Journal of Aerospace Engineering*. 1–12 (2018). <https://doi.org/10.1155/2018/9570873> URL: <https://www.hindawi.com/journals/ijae/2018/9570873/>
4. Pang, S., Li, Q., Ni, B.: Improved nonlinear MPC for aircraft gas turbine engine based on semi-alternative optimization strategy. *Aerospace Science and Technology* 118, 106983 (2021). <https://doi.org/10.1016/j.ast.2021.106983>
5. Shen, Y., Khorasani, K.: Hybrid multi-mode machine learning-based fault diagnosis strategies with application to aircraft gas turbine engines. *Neural Networks* 130, 126–142 (2020). doi: <https://doi.org/10.1016/j.neunet.2020.07.001>
6. Filippone, A., Zhang, M., Bojdo, N.: Validation of an integrated simulation model for aircraft noise and engine emissions. *Aerospace Science and Technology* 89, 370–381 (2019). <https://doi.org/10.1016/j.ast.2019.04.008>
7. Cai, C., Wang, Y., Fang, J., Chen, H., Zheng, Q., Zhang H.: Multiple aspects to flight mission performances improvement of commercial turbofan engine via variable geometry adjustment. *Energy* 263(A), 125693 (2023). <https://doi.org/10.1016/j.energy.2022.125693>
8. de Voogt, A., St. Amour, E.: Safety of twin-engine helicopters: Risks and operational specificity. *Safety Science* 136, 105169 (2021). doi: 10.1016/j.ssci.2021.105169
9. Li, Y., Xuan, Y.: Thermal characteristics of helicopters based on integrated fuselage structure/engine model. *International Journal of Heat and Mass Transfer* 115(A), 102–114 (2017). <https://doi.org/10.1016/j.ijheatmasstransfer.2017.07.038>
10. Sheng, H., Chen, Q., Li, J., Jiang, W., Wang, Z., Liu, Z., Zhang, T., Liu, Y.: Research on dynamic modeling and performance analysis of helicopter turboshaft engine's start-up process. *Aerospace Science and Technology* 106, 106097 (2020). <https://doi.org/10.1016/j.ast.2020.106097>
11. Infante, V., Freitas, M.: Failure analysis of compressor blades of a helicopter engine. *Engineering Failure Analysis* 104, 67–74 (2019). <https://doi.org/10.1016/j.engfailanal.2019.05.024>

12. Chen, Y.-Z., Tsoutsanis, E., Wang, C., Gou, L.-F.: A time-series turbofan engine successive fault diagnosis under both steady-state and dynamic conditions. *Energy* 263(D), 125848 (2023). <https://doi.org/10.1016/j.energy.2022.125848>
13. Andoga, R., Fozo, L., Schrotter, M., Ceskovic, M.: Intelligent thermal imaging-based diagnostics of turbojet engines. *Applied Sciences* 9(11), 2253 (2019). <https://doi.org/10.3390/app9112253>
14. Kuznetsova, T., Likhacheva, Y., Gubarev, E., Yakushev, A.: The identification of gas turbine engine parameters by the multidimensional Kalman filter. *Electrical engineering, information technology, control systems* 10, 114–126 (2014).
15. Vladov, S., Shmelov, Y., Yakovliev, R.: Modified Helicopters Turbohaft Engines Neural Network On-board Automatic Control System Using the Adaptive Control Method. ITTAP'2022: 2nd International Workshop on Information Technologies: Theoretical and Applied Problems, November 22–24, 2022, Ternopil, Ukraine. *CEUR Workshop Proceedings (ISSN 1613-0073)* 3309, 205–229 (2022).
16. Karvonen, T., Bonnabel, S., Moulines, E., Sarkka, S.: On stability of a class of filters for nonlinear stochastic systems. *SIAM Journal on Control and Optimization* 58(4), 2023–2049 (2020). <https://doi.org/10.1137/19M1285974>
17. Jia, C., Hu, J.: Variance-constrained filtering for nonlinear systems with randomly occurring quantized measurements: recursive scheme and boundedness analysis. *Advances in Difference Equations* 2019.53, (2019). <https://doi.org/10.1186/s13662-019-2000-0>. URL: <https://d-nb.info/1180488768/34>
18. Long, Z., Bai, M., Ren, M., Liu, J., Yu, D.: Fault detection and isolation of aeroengine combustion chamber based on unscented Kalman filter method fusing artificial neural network. *Energy* 1, 127068 (2023). <https://doi.org/10.1016/j.energy.2023.127068>
19. Kellermann, C., Ostermann, J.: Estimation of unknown system states based on an adaptive neural network and Kalman filter. *Procedia CIRP* 99, 656–661 (2021). <https://doi.org/10.1016/j.procir.2021.03.089>
20. Togni, S., Nikolaidis, T., Sampath, S.: A combined technique of Kalman filter, artificial neural network and fuzzy logic for gas turbines and signal fault isolation. *Chinese Journal of Aeronautics* 34(2), 124–135 (2021). <https://doi.org/10.1016/j.cja.2020.04.015>
21. Shmelov, Y., Vladov, S., Klimova, Y., Kirukhina, M.: Expert system for identification of the technical state of the aircraft engine TV3-117 in flight modes. *System Analysis & Intelligent Computing: IEEE First International Conference on System Analysis & Intelligent Computing (SAIC)*, 08–12 October, 77–82 (2018). <https://doi.org/10.1109/SAIC.2018.8516864>
22. Chernodub, A.: Training of Neuroemulators with Use of Pseudoregularization for Model Reference Adaptive Neurocontrol. *Artificial intelligence* 4, 602–614 (2012).
23. Gyamfi, K. S., Brusey, J., Gaura, E.: Differential radial basis function network for sequence modelling. *Expert Systems with Applications* 189, 115982 (2022). <https://doi.org/10.1016/j.eswa.2021.115982>
24. Sideratos, G., Hatzigiorgiou, N. D.: A distributed memory RBF-based model for variable generation forecasting. *International Journal of Electrical Power & Energy Systems* 120, 106041 (2020). <https://doi.org/10.1016/j.ijepes.2020.106041>
25. Vladov, S., Shmelov, Y., Yakovliev, R., Petchenko, M., Drozdova, S.: Neural Network Method for Helicopters Turbohaft Engines Working Process Parameters Identification at Flight Modes. 2022 IEEE 4th International Conference on Modern Electrical and Energy System (MEES), Kremenchuk, Ukraine, October 20–22, 2022, 604–609 (2022). <https://doi.org/10.1109/MEES58014.2022.10005670>

26. Puchkov, A., Dli, M., Lobaneva, E., Vasilkova, M.: Predicting an object state based on applying the Kalman filter and deep neural networks, *Software & Systems*, 32(3), 368–376 (2019). <https://doi.org/10.15827/0236-235X.127.368-376>.
27. Vladov, S., Shmelov, Y., Yakovliev, R.: Modified Method of Identification Potential Defects in Helicopters Turboshaft Engines Units Based on Prediction its Operational Status. 2022 IEEE 4th International Conference on Modern Electrical and Energy System (MEES), Kremenchuk, Ukraine, October 20–22, 2022, 556–561 (2022). <https://doi.org/10.1109/MEES58014.2022.10005605>
28. Vladov, S., Shmelov, Y., Yakovliev, R. Methodology for Control of Helicopters Aircraft Engines Technical State in Flight Modes Using Neural Networks, The Fifth International Workshop on Computer Modeling and Intelligent Systems (CMIS-2022), May, 12, 2022, Zaporizhzhia, Ukraine, CEUR Workshop Proceedings (ISSN 1613-0073), 3137, 108–125 (2022). <https://doi.org/10.32782/cmisis/3137-10>
29. Yoo, H.-M., Park, M.-K., Park, B.-G., Lee, J.-H.: Effect of layer-specific synaptic retention characteristics on the accuracy of deep neural networks, *Solid-State Electronics* 200, 108570 (2023). <https://doi.org/10.1016/j.sse.2022.108570>
30. Saneifard, R., Jafarian, A., Ghalami, N., Measoomy Nia, S.: Extended artificial neural networks approach for solving two-dimensional fractional-order Volterra-type integro-differential equations, *Information Sciences* 612, 887–897 (2022). <https://doi.org/10.1016/j.ins.2022.09.017>
31. Shamlitskiy, Y., Popov, A., Saidov, N., Moiseeva, K.: Transport Stream Optimization Based on Neural Network Learning Algorithms, *Transportation Research Procedia* 68, 417–425 (2023). <https://doi.org/10.1016/j.trpro.2023.02.056>
32. Wei, W., Chuan, J.: A combination forecasting method of grey neural network based on genetic algorithm, *Procedia CIRP* 109, 191–196 (2022). <https://doi.org/10.1016/j.procir.2022.05.235>
33. Hu, X., Wei, X., Gao, Y., Liu, H., Zhu, L.: Variational expectation maximization attention broad learning systems, *Information Sciences* 608, 597–612 (2022). <https://doi.org/10.1016/j.ins.2022.06.074>
34. Pattnaik, M., Badoni, M., Tatte, Y.: Application of Gaussian-sequential-probabilistic-inference concept based Kalman filter for accurate estimation of state of charge of battery, *Journal of Energy Storage* 54, 105244 (2022). <https://doi.org/10.1016/j.est.2022.105244>
35. Lu, F., Gao, T., Huang, J., Qiu, X.: Nonlinear Kalman filters for aircraft engine gas path health estimation with measurement uncertainty, *Aerospace Science and Technology* 76, 126–140 (2018). <https://doi.org/10.1016/j.ast.2018.01.024>
36. Cordeiro, R. A., Azinheira, J. R., Moutinho, A.: Actuation Failure Detection in Fixed-Wing Aircraft Combining a Pair of Two-Stage Kalman Filters, *IFAC-PapersOnLine* 53(2), 7144–749 (2020). <https://doi.org/10.1016/j.ifacol.2020.12.825>